

AD-A086 218

ROYAL AIRCRAFT ESTABLISHMENT FARNBOROUGH (ENGLAND)

F/6 20/11

GREEN'S FUNCTIONS IN FRACTURE MECHANICS.(U)

MAR 80 D J CARTWRIGHT, D P ROOKE

UNCLASSIFIED

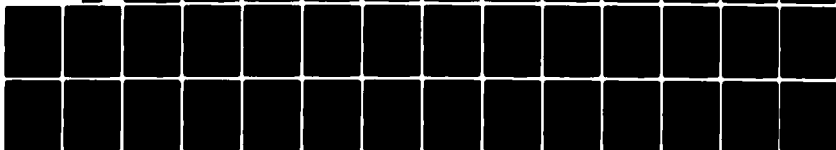
RAE-TR-80035

DRIC-BR-74344

NL

1.51  
25.000000

1



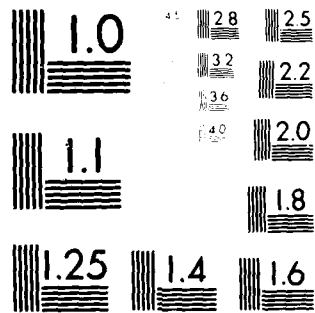
END

DATE

FILED

80-801

DTIC



MICROCOPY RESOLUTION TEST CHART  
NATIONAL BUREAU OF STANDARDS-1963-A

TR 80035

TR 80035

**LEVEL**  
UNLIMITED



2  
R

ROYAL AIRCRAFT ESTABLISHMENT

\*

Technical Report 80035

March 1980

# GREEN'S FUNCTIONS IN FRACTURE MECHANICS

by

D.J. Cartwright  
D.P. Rooke

DTIC  
ELECTE  
AUG 21 1980  
C

\*

Procurement Executive, Ministry of Defence  
Farnborough, Hants

DDC FILE COPY

UNLIMITED

80 8 15 120

(14) RAE-TR-80035

(2)

UDC 539.4.014.11 : 517.956.225 : 539.211

(11) Ma 84

(12) 44

ROYAL AIRCRAFT ESTABLISHMENT

(9) Technical Report, 80035

Received for printing 5 March 1980

(6) GREEN'S FUNCTIONS IN FRACTURE MECHANICS.

by

(10) D. J. Cartwright\*  
D. P. Rooke

(18) DRIC

SUMMARY

(19) BR-74374

The use of Green's functions in the determination of stress intensity factors is described and applied to the solution of problems in fracture mechanics. Methods of obtaining further Green's functions from existing ones are presented. It is shown that several commonly used simple methods of determining stress intensity factors can be expressed in terms of approximate Green's functions. Many important Green's functions are presented and some of these are used to solve several problems of practical importance to the aerospace industry, eg cracks in stiffened sheets and cracks in pin-loaded lug-joints.

*This paper was presented as a lecture to a conference on Fracture Mechanics: Current Status, Future Prospects held at Cambridge, 16 March 1979. Proceedings edited by R.A. Smith, published Pergamon 1979.*

Departmental Reference: Mat 394

Copyright  
©

Controller HMSO London  
1980

REC  
AUG 21 1980

\* A Senior Lecturer from the Department of Mechanical Engineering, University of Southampton.

310450 Jm

LIST OF CONTENTS

	<u>Page</u>
1 INTRODUCTION	3
2 BASIC PRINCIPLES OF GREEN'S FUNCTIONS	3
3 STRESS INTENSITY FACTORS AS GREEN'S FUNCTIONS	4
4 SYSTEMATIC USE OF GREEN'S FUNCTIONS	5
5 AVAILABLE GREEN'S FUNCTIONS	8
6 SIMPLE METHODS EXPRESSED AS GREEN'S FUNCTIONS	8
7 APPLICATIONS OF GREEN'S FUNCTIONS	12
7.1 Effect of pin pressure distribution on a crack at a hole	12
7.2 Crack with a strip-yield zone in a stiffened sheet	13
7.3 A symmetrical crack in a stiffened sheet	15
8 CONCLUSIONS	16
References	17
Illustrations	Figures 1-18
Report documentation page	inside back cover

Accession For	
NTIS GNA&I	<input checked="" type="checkbox"/>
DDC TAB	<input type="checkbox"/>
Unannounced	<input type="checkbox"/>
Justification	<input type="checkbox"/>
By _____	
Distribution/	
Availability Codes	
Dist.	Avail and/or special
A	

## 1 INTRODUCTION

Many theoretical (analytical and numerical) and experimental methods for evaluating stress intensity factors are now available; they have been described in several reviews, for example, Refs 1, 2 and 3. Techniques involving Green's functions have been used for determining stress intensity factors of cracks under complex loading conditions. These techniques, which offer scope for further development, are discussed in this paper in relation to two areas where they are of particular use. The first is in the systematic use of a known Green's function to develop one for a more complex configuration. The second is the development of engineering methods of evaluating stress intensity factors by approximating Green's functions.

Some applications are described of these techniques to problems of general engineering interest such as cracks at loaded holes and cracks in stiffened structures. The Green's functions developed give an insight into the importance of different types of loading and structure and demonstrate the versatility of the technique. Some of the more useful Green's functions are discussed in section 5.

## 2 BASIC PRINCIPLES OF GREEN'S FUNCTIONS

The Green's function, first postulated by George Green in 1828, is defined as the response of a system to a standard input. The standard input is usually in the form of an impulse. Stedman<sup>4</sup> has reviewed the use of Green's functions in many fields of mathematical physics. Some examples of classical Green's functions are: the voltage output, as a function of time, of an electronic circuit in response to an input voltage pulse; the dynamic response of a mechanical system set in motion by an impulsive blow; the stress field produced in an elastic body in response to a force acting at a point in the body. If the body in the last example contains a crack, the stress intensity factor at the crack tip which arises in response to the point force may be considered as a special case of a Green's function. The important property of these functions is that, when suitably defined, they contain all the essential information about the system. They can thus be used to obtain the response of the system to any input by considering it as being composed of large numbers of small impulses. The total response is the sum of all the individual responses due to each input impulse acting separately. For the Green's function representation to be valid the system must have the following properties:

- (a) causality - if there is no input there is no response;
- (b) invariance - the response to a given input is always the same;

- (c) linearity - if the response to input  $I_1$  is  $R_1$  and the response to  $I_2$  is  $R_2$  then the response to  $I_1 + I_2$  is  $R_1 + R_2$ .

These three conditions lead to the following result for the response  $R(\eta)$  to a general input  $I(\eta)$ .

$$R(\eta) = \int I(\eta)G(\eta - \eta')d\eta' \quad (1)$$

where  $G(\eta - \eta')$  is defined as the Green's function and is a function of the differences  $\eta - \eta'$ . The variables  $\eta$  and  $\eta'$  may represent positions and/or time.

### 3 STRESS INTENSITY FACTORS AS GREEN'S FUNCTIONS

The stress intensity factor is known<sup>5</sup> for the two-dimensional problem of a cracked sheet containing a crack of length  $2a$  which has localized forces acting at points on its surfaces (see Fig 1). If the forces act normal to the crack faces, i.e. a force per unit thickness of  $P$  acting on one face and an equal and opposite force acting on the other face, then the opening mode stress intensity factor  $K_I$  at tip A is given by

$$K_I = \frac{P}{\sqrt{\pi a}} \left[ \frac{a + x_0}{a - x_0} \right]^{\frac{1}{2}} \equiv \frac{P}{\sqrt{\pi a}} G(x_0) \quad (2)$$

where  $x_0$  is the distance of the point of application of the force from the centre of the crack. If forces  $Q$  act tangentially to the crack faces then the sliding-mode stress intensity factor  $K_{II}$  at tip A is given by

$$K_{II} = \frac{Q}{\sqrt{\pi a}} \left[ \frac{a + x_0}{a - x_0} \right]^{\frac{1}{2}} \equiv \frac{Q}{\sqrt{\pi a}} G(x_0) \quad (3)$$

For tip B at the other end of the crack the stress intensity factors are obtained from equations (2) and (3) by replacing  $x_0$  with  $-x_0$ . The function  $G(x_0)$  in equations (2) and (3) can be used as a Green's function to obtain stress intensity factors for cracks subjected to boundary pressures acting on the crack faces. If a pressure  $p(x)$ ,  $-a \leq x \leq a$ , acts normal to the crack faces the stress intensity factor is given by

$$K_I = \frac{1}{\sqrt{\pi a}} \int_{-a}^a p(x)G(x)dx \quad (4)$$

For the case of  $p(x) = p$  (a constant), equation (3) gives the well known result  $K_I = p\sqrt{\pi a}$ . A similar result can be obtained for a distribution of shearing forces on the crack. For symmetrical point forces on the crack faces the pressure distribution can be represented by  $p(x) = P\delta(x - x_0)$  where  $\delta(x - x_0)$  is the Dirac delta function. Substitution of this expression for  $p(x)$  reduces equation (4) to equation (2).

Equation (3) can be used together with an important result derived by Bueckner<sup>6</sup>, to obtain opening mode stress intensity factors for cracked bodies subjected to arbitrary forces on their boundaries. Bueckner's result is that the stress intensity factor for a crack in a body subjected to external forces is identical to that for a similar crack, subjected to internal pressure in a similar body which has no external forces acting on it. The internal pressure  $p(x)$  acting in the crack is equal to the stress that would exist normal to the crack-line along the crack-site in the uncracked body subjected to the external forces. An analogous procedure exists for shear stresses and the calculation of sliding-mode stress intensity factors. This principle is illustrated schematically in Fig 2. For many bodies and external force distributions the stresses along the crack-site may be difficult to evaluate. Often Green's function techniques can be used in these evaluations. Recently Nisitani<sup>7</sup> has derived stress-field Green's functions for different bodies, so that the internal stress distribution can be derived for any externally applied forces on these bodies.

#### 4 SYSTEMATIC USE OF GREEN'S FUNCTIONS

Known Green's functions for both stress fields and stress intensity factors can often be used systematically to build up stress intensity factors for unsolved crack problems. Some examples are shown in Fig 3 where  $G^K$  and  $G^\sigma$  refer to Green's functions which are associated with stress intensity factors and stress fields respectively. The Green's function defined in equation (3) is a special case of that derived by Erdogan<sup>8</sup> for a crack in a sheet with an arbitrary force anywhere in the sheet. The stress-field Green's functions are also available<sup>8</sup> for this cracked configuration. The ones required are defined in Fig 3b. Hartranft and Sih<sup>9</sup> have obtained the stress intensity factor for a crack of length  $a$  in a half-plane, the crack being subjected to two equal and opposite forces (per unit thickness)  $P$ , normal to the crack face and a distance  $x_0$  from the edge of the

sheet (see Fig 3c). An iterative method was used which required a knowledge of the Green's functions given in Figs 3a&b. The initial solution required was that of a crack of length  $2a$  with point forces  $\pm P$  at  $x = \pm x_0$ ; the Green's functions for this configuration are obtained from Fig 3b, i.e.

$$K_I = \frac{P}{\sqrt{\pi a}} \left[ G_B^K(x_0; a) + G_B^K(-x_0; a) \right] , \quad (5)$$

$$\sigma_x(y, 0) = P \left[ G_B^\sigma(x_0, y; a) + G_B^\sigma(-x_0, y; a) \right] = 2PG_B^K(x_0, y; a) , \quad (6)$$

$$\tau_{xy}(y, 0) = P \left[ G_B^\tau(x_0, y; a) + G_B^\tau(-x_0, y; a) \right] = 0 . \quad (7)$$

The simplifications introduced into equations (6) and (7) follow from symmetry considerations.

The configuration described in Fig 3d can be solved directly from equation (4) by using the above solution. Because of Bueckner's principle<sup>6</sup>  $p(x)$  can be replaced by  $\sigma_y(x, 0)$ , defined in Fig 3a, and  $G(x)$  can be replaced by  $G_C^K(x_0; a)$  defined in Fig 3c. This procedure has been used by Rooke and Jones<sup>10</sup> to obtain the desired solution. Fig 3f shows a crack of length  $a$  in a half-plane which is subjected to a force per unit thickness of  $P$  acting at the point  $(x_0, y_0)$ . The stress intensity factor for this configuration can be obtained in a similar manner to that above from the Green's functions defined in Fig 3c&e. The result  $G_F^K(x_0, y_0; a)$  can then be used to derive the stress intensity factor for any arbitrary distribution of forces in the half-plane. All the configurations in Fig 3 show opening mode stress intensity factors resulting from forces normal to the crack or normal to the sheet edge. The procedures outlined are also valid for arbitrary forces which lead to both opening and sliding-mode stress intensity factors.

Stress intensity factors for cracks subjected to a constant pressure on part of the crack surface are closely related to Green's functions. A particular case of this is illustrated in Fig 4a where a crack of length  $2a$  is subjected to a constant pressure.  $p(x) = p_0$  between  $x_0 \leq x \leq x_1$ . Symbolically  $p(x)$  is defined as

$$p(x) = p_0 \left[ H(x - x_0) - H(x - x_1) \right] \quad (8)$$

where  $H(x - x_0)$  is the Heaviside step-function defined by

$$\left. \begin{aligned} H(x - x_0) &= 0 & x < x_0 \\ &= 1 & x \geq x_0 \end{aligned} \right\} \quad (9)$$

The Heaviside step-function and the Dirac delta-function are simply related thus:

$$\frac{d}{dx} H(x - x_0) = \delta(x - x_0) \quad (10)$$

From equation (4) it follows that the stress intensity factor for the configuration is given by

$$K_I = \frac{p_0}{\sqrt{\pi a}} \int_{-a}^a [H(x - x_0) - H(x - x_1)] G(x) dx = \frac{p_0}{\sqrt{\pi a}} \int_{x_0}^{x_1} G(x) dx \quad (11)$$

where  $G(x)$  is defined by equation (2); the second integral in equation (11) follows from the properties of  $H(x)$  given in equation (9). This result can be used to obtain an approximate stress intensity factor for a crack subjected to an arbitrary pressure distribution. The pressure distribution is approximated by a series of strips of constant pressure as illustrated in Fig 4b. The principle of superposition allows the contributions from each pressure strip to be added together. Thus

$$K_I = \frac{p_1}{\sqrt{\pi a}} \int_{x_0}^{x_1} G(x) dx + \frac{p_2}{\sqrt{\pi a}} \int_{x_1}^{x_2} G(x) dx + \dots + \frac{p_n}{\sqrt{\pi a}} \int_{x_{n-1}}^{x_n} G(x) dx \quad (12)$$

where  $p_j$  is the value of  $p(x)$  at the mid-point of the strip between  $x_{j-1}$  and  $x_j$ .

If each strip is of such a width that  $p(x)$  does not vary much across it, then equation (12) may be written

$$K_I = \frac{1}{\sqrt{\pi a}} \left\{ \int_{x_0}^{x_1} p(x) G(x) dx + \int_{x_1}^{x_2} p(x) G(x) dx + \dots + \int_{x_{n-1}}^{x_n} p(x) G(x) dx \right\} \quad (13)$$

By adding the integrals together, equation (13) becomes

$$K_I \approx \frac{1}{\sqrt{\pi a}} \int_{x_0}^{x_n} p(x)G(x)dx, \quad (14)$$

the right-hand side of which is of the same form as equation (4); for a distribution of pressure over the whole crack-face  $x_0$  is  $-a$  and  $x_n$  is  $+a$ . Thus equation (12) will give results which approximate to those of an exact calculation using Green's functions, providing that  $p(x)$  does not vary much in any strip. The number of strips can be increased indefinitely until the stress intensity factor reaches the required accuracy.

##### 5 AVAILABLE GREEN'S FUNCTIONS

There are many Green's functions now available. The more important of these are shown in Fig 5. Most are for two-dimensional configurations and these enable a wide variety of problems to be analysed. The Green's functions shown are mainly for Modes I and II as these are in practice more important. Complete details of the functions together with references to the original work are given in the references cited for each configuration. Many other special cases of the Green's functions in Fig 5 have been determined<sup>11-13</sup>, and it is possible to construct others by taking limits and by superposition. Solutions have also been determined<sup>11-13</sup> for bands of pressure on the crack faces and, as shown by equation (14), these step-function solutions can be superimposed to obtain arbitrary distributions on the crack surfaces.

##### 6 SIMPLE METHODS EXPRESSED AS GREEN'S FUNCTIONS

Several simple methods<sup>14-18</sup> have been proposed for determining stress intensity factors, particularly for the important case of cracks from holes or notches. These methods have been developed by comparing results with known stress intensity factors in particular cases. It will now be shown that these simple methods are not arbitrary, but arise from approximations to the Green's function. Results obtained from using them will be compared with those derived by Hsu and Rudd<sup>19</sup> who used a more accurate Green's function. Hsu and Rudd determined stress intensity factors for a symmetrical pair of opposing point forces acting on each of two radial cracks of length  $l$  at a hole of radius  $R$  (see Fig 6). They used finite element methods for  $x/l < 0.9$  and a limiting expression for  $x/l > 0.9$ . The Green's function given by Hsu and Rudd is shown

(solid curves) in Fig 7 for three values of  $\ell/R = 0.2, 1.0$  and  $3.0$ . Two features of the Green's function are of special interest; it is a weak function of  $\ell/R$  and it tends to infinity as the point force approaches the crack tip. Green's functions for an edge crack<sup>9,11</sup> depicted in Fig 8 and an embedded crack<sup>8</sup> depicted in Fig 9 are also shown in Fig 7.

The Green's function for the edge crack is given<sup>9</sup> as

$$G_e(X) = \frac{2}{\sqrt{1-X^2}} \left\{ 1 + (1-X^2) \left[ 0.2945 - 0.3912X^2 + 0.7685X^4 - 0.9942X^6 + 0.5094X^8 \right] \right\} \quad (15)$$

and for the embedded crack from equation (2) by superposition as

$$G_c(X) = \frac{2}{\sqrt{1-X^2}} \quad (16)$$

where  $X = x/\ell$ .

The Green's function of Hsu and Rudd lie close to equations (15) and (16) for  $X \rightarrow 1$ . Shah has developed a method<sup>17,18</sup> by considering the limiting behaviour of known stress intensity factors for cracks at holes. When expressed as a Green's function the method reduces to using

$$G_s(X) = \frac{2M_f}{\sqrt{1-X^2}} \quad (17)$$

$$\begin{aligned} \text{where } M_f &= 1.0 + 0.12 \left\{ \frac{X - 0.3}{0.3} \right\}^2; & X < 0.3 \\ &= 0; & X > 0.3 \end{aligned}$$

This Green's function is also shown in Fig 7 and can be seen to be a reasonable approximation to that of Hsu and Rudd. The free surface correction factor  $M_f$  was introduced by Shah to take approximate account of the stress-free hole-boundary which affects the stress intensity factor at short crack lengths. The limiting value of  $M_f (= 1.12)$  is the value obtained for a crack at the edge of a uniformly stressed half-plane. The approximate Green's function proposed by Shah is sufficiently close to the solution of Hsu and Rudd to make it useful for many applications; its use does not depend on the notch shape and a closed form expression is convenient in numerical calculations.

The approximate methods<sup>14-16</sup> can also be expressed as Green's functions thereby establishing their general application to cracks at holes and notches. The Green's function  $G_0(x)$  for a point loaded crack at a notch tip as shown in Fig 10a is shown schematically in Fig 10b. Three approximations to  $G_0(x)$  will be examined, these are also shown in Fig 10b and are defined as

$$G_1(x) = 1.12\pi\ell\delta(x) , \quad (18)$$

$$G_2(x) = 1.12\pi\ell\delta(x - \ell) \quad (19)$$

and

$$G_3(x) = 1.12\pi [H(x) - H(x - \ell)] \quad (20)$$

where  $\delta(x)$  is the Dirac delta-function,  $H(x)$  is the Heaviside step-function. It will now be shown that the above Green's functions are equivalent to well known results.

From equation (4) the stress intensity factors resulting from the Green's functions in equations (18) to (20), with  $\sigma(x)$ , the stress over the crack site, set equal to  $p(x)$  are given by:

for equation (18)

$$K_I^{(1)} = \frac{1}{\sqrt{\pi\ell}} \int_0^\ell \sigma(x) 1.12\pi\ell\delta(x) dx \quad (21)$$

$$= 1.12\sigma(0)\sqrt{\pi\ell} ; \quad (22)$$

for equation (19)

$$K_I^{(2)} = \frac{1}{\sqrt{\pi\ell}} \int_0^\ell \sigma(x) 1.12\pi\ell\delta(x - \ell) dx \quad (23)$$

$$= 1.12\sigma(\ell)\sqrt{\pi\ell} ; \quad (24)$$

and for equation (20)

$$K_I^{(3)} = \frac{1}{\sqrt{\pi\ell}} \int_0^\ell \sigma(x) 1.12\pi [H(x) - H(x - \ell)] dx \quad (25)$$

$$= 1.12\sqrt{\pi\ell} \left\{ \frac{1}{\ell} \int_0^{\ell} \sigma(x) dx \right\} \quad (26)$$

$$= 1.12\sigma_{\text{mean}}\sqrt{\pi\ell} \quad (27)$$

Equations (22) and (24) are the familiar maximum stress<sup>16</sup> and crack tip stress<sup>14</sup> approximations respectively and equation (27) is the mean stress method suggested by Williams and Isherwood<sup>15</sup>; several applications of these methods have been considered elsewhere<sup>3</sup>.

Results for the case of two equal length, diametrically opposed, radial cracks at a hole in a sheet subjected to a biaxial tensile stress  $\sigma$  are shown in a table in Fig 11. For this case

$$\sigma(x) = \sigma \left( 1 + \frac{R^2}{(R+x)^2} \right) \quad (28)$$

The results of Hsu and Rudd<sup>19</sup> as determined by Whitehead<sup>20</sup> are seen to be in close agreement with the accurate solution of Rooke and Tweed<sup>21</sup>; errors for each approximation are shown in parenthesis. The tip stress equation (24), results in errors of about 3% showing that the Green's function  $G_1(x)$  is a satisfactory approximation to  $G_0(x)$ . This is because the major contribution to the stress intensity factor comes from the near tip stresses; this contribution is largely accounted for by the delta function representation of the Green's function. The maximum stress approximation is only accurate in the limit of zero crack length as only under these conditions is the delta function  $\delta(x)$  a reasonable approximation to  $G_0(x)$ . However despite this limitation the maximum stress method is useful in that it gives an upper limit on the stress intensity factor. Furthermore it is only necessary to know the stress concentration factor for the notch rather than the entire stress field over the crack-site in the uncracked body. The mean stress method also over-estimates the stress intensity factor but in this case it is necessary to know the entire stress field over the crack-site and to determine its mean value at each crack length. Smith<sup>22</sup> has made use of the mean stress and the properties of Green's functions to establish bounds on stress intensity factors of edge cracks when  $\sigma(x)$  is a monotonically decreasing function and  $\sigma(\ell) > 0$ .

## 7 APPLICATIONS OF GREEN'S FUNCTIONS

The usefulness of Green's functions in fracture mechanics will now be illustrated by three examples. These are chosen to illustrate the wide variety of practical problems which may be easily and accurately solved.

### 7.1 Effect of pin pressure distribution on a crack at a hole

In this example it is necessary to give a different interpretation to  $p(x)$  and  $G(x)$  in equation (4) since in order to solve these problems we need the Green's function which gives the response to a force acting at an arbitrary position in the body (in this case on the hole boundary) rather than that due to a force acting on the crack surfaces. For problems of this type the stress intensity factor for an arbitrary stress acting on the body is obtained from the following expression which is similar to equation (4)

$$K_I = \frac{1}{\sqrt{\pi l}} \int_{x_1}^{x_2} \sigma(x) G(x) dx \quad (29)$$

where  $x_1$  and  $x_2$  are positions in the body between which  $\sigma(x)$  is the applied stress prescribed and  $G(x)$  is the stress intensity factor for a unit force acting at the position denoted by  $x$ . As an example of the use of such Green's functions we will consider a radial crack at the edge of a circular hole which is subjected to a point force on its perimeter. This type of problem is frequently encountered in considering cracked-holes in pin-loaded lugs. Often the load transfer between the pin and the hole periphery is not precisely known and it is necessary to investigate various possible load distributions. Green's function techniques are ideal for such investigations since each new distribution just involves a change in  $\sigma(x)$  in equation (29).

The Green's function required is the stress intensity factor for a radial crack of length  $l$  at the edge of a hole of radius  $R$ ; a radial force per unit thickness of  $P$  acts at the edge of the hole in a direction which makes an angle  $\theta$  with the crack (see Fig 12). This stress intensity factor has been obtained by Tweed and Rooke<sup>23</sup>; it is plotted in Fig 12 in non-dimensional form as a function of  $\theta$  for various values of  $l/R$ . The usefulness of Green's functions in describing the response of systems is clearly shown by these results since two important observations can be made from Fig 12. The first is that the variation of  $K_I$  with  $\theta$  increases as the crack length decreases, and the second is that

the maximum rate of variation occurs for short cracks at small values of  $\theta$ . These facts lead to important considerations in fracture mechanics applications.

The first consideration, which is of general importance, is that since most of the lifetime of a fatigue crack is spent while the crack is short, it is necessary to know what influences the stress intensity factor of short cracks. This information is required in order to decide on inspection intervals and maintenance schedules for structures in services. The second consideration is specific to the loaded hole configuration since assumptions have usually to be made about how the load is transferred from the pin to the edge of the hole. It is often assumed that the load is distributed, in some way, between  $\theta_1$  and  $\theta_2$  where  $\theta_1 \sim 0^\circ$  and  $\theta_2 \sim 180^\circ$ . The rapid variation in Green's function at small values of  $\theta$  means that an incorrect assumption of the load distribution and the cut-off value  $\theta_1$  can lead to significant errors in the stress intensity factor. The errors will be largest for the important region of short cracks, so great care must be exercised in simulating the load transfer between the pin and the edge of the hole.

## 7.2 Crack with a strip-yield zone in a stiffened sheet

Green's functions have been used extensively to analyse the effect of cracks in stiffened structures. The stiffener may be discretely attached<sup>24</sup> *eg* riveted or spot welded, or it may be continuously attached<sup>25</sup>, *eg* bonded or integrally machined. Multiple stiffeners have been studied<sup>26</sup> and the effect of attachment deflection, *eg* distortion of adhesives or rivets has been analysed<sup>27,28</sup>. By using the same method it is also possible to determine the effect of repair patches<sup>29</sup> and the effect of debonding of the adhesive<sup>30</sup>. In this example a recently reported method<sup>31</sup> is used to examine the effect of yielding at the tip of a crack in a stiffened panel. Such problems arise in the residual static strength assessment of stiffened structures because of the relatively high loads involved. It is therefore necessary to consider the effect of yielding in the sheet on the load concentration in the stiffener and on the rivet loads. We must also consider the deflection of the attachment points, possible fracture of the attachments and the crack opening displacement of the crack.

In the configuration analysed, shown in Fig 13, a sheet of modulus of elasticity  $E$ , thickness  $t$  and yield stress  $\sigma_{ys}$  is stiffened by a line-stiffener of area  $A_s$  and modulus of elasticity  $E_s$ . The stiffener is attached to the sheet by  $N$  rivets (symmetrically either side of the crack) of elastic compliance  $q$  spaced a distance  $p$  apart. A crack of length  $2a$  is located symmetrically across the stiffener and has a strip-yield zone of length  $c$  at

each tip; the sheet is subjected to a uniaxial stress  $\sigma$  perpendicular to the crack. It is assumed that the attachment points are either rigid ( $Etq = 0$ ) or undergo an elastic deflection typical of thin sheet riveted structures ( $Etq = 3$ ).

The stiffened panel in Fig 13 has been analysed using the Green's function<sup>8</sup> (see also Fig 5a). In solving problems of this type a series of compatibility equations are set up; these relate the extension of each attachment interval in the sheet to that of the contiguous interval in the stiffener. This gives a set of simultaneous equations which may be solved for the unknown attachment forces. Once these are known the effect of each attachment force may be summed using a displacement Green's function to obtain the crack opening displacement of the crack. Convergence of the solution is established by increasing the number of rivets in the stiffener until there is no effect on the attachment force distribution. On this basis the number of attachments  $N$  was fixed at 30 either side of the crack line.

We consider a problem in which the extent of yielding in the sheet is limited to a length  $c$  equal to the crack length  $a$ . In practice this could correspond to a half-bay crack in a multi-stiffened panel where yielding is not permitted to extend past the next stiffener either side of the crack. The following aspects of the problem have been studied in detail, the effect of attachment failure on the maximum attachment load, the load concentration in the stiffener and the crack opening displacement. The influence of increasing the number,  $n$ , of failed attachment points is shown in Fig 14. The crack opening displacement  $\delta$  and the strip-yield zone length  $c$  are both reduced below that for an unstiffened sheet ( $\delta_0, c_0$ ) and increase monotonically with increasing  $n$ . The ratio of the maximum permissible applied stress  $\sigma$  to the strip-yield stress  $\sigma_{ys}$  appears to be only weakly affected by the number of failed attachment points. The reduction in  $\sigma/\sigma_{ys}$  show that the panel can carry less load for the same yield zone length. The ratio of the maximum stress  $\sigma_m$  in the stiffener to the remote stiffener stress  $\sigma_s$  decreases by approximately 22%. The ratio of the load  $P_1$  in the unbroken attachment nearest to the crack to the remote load in the stiffener  $\sigma_s A_s$  shows an increase initially followed by a decrease of approximately 37% compared to the initial value.

It is instructive to compare the maximum rivet load and the maximum stress in the stiffener for the strip-yield crack with that of a crack having the same length  $a$  but without a strip-yield zone at its tip. This is shown in Fig 15, where it is seen that the effect of yielding is to increase the maximum rivet load by between 9% and 26% whilst the maximum stress in the stiffener increases by

only 6%. The implications of this are that the effect of yielding in the sheet is more likely to cause further shear deflection, yield or failure of the rivets rather than yield or failure of the stiffener. In Fig 16 the effect of attachment deflection on the crack opening displacement  $\delta$ , maximum stiffener stress  $\sigma_m$  and maximum rivet load  $P_1$  are shown as a function of the number of the failed attachment points. The attachment deflection has the effect of increasing the crack opening displacement. It is increased by approximately 32% when all attachments are intact and by 10% when eight are broken. The maximum stiffener stress is reduced by only about 6% whereas the maximum rivet load is significantly reduced by approximately 60%, both being relatively insensitive to  $n$ . Further details of the application of Green's functions to cracks with strip-yield zones in stiffened sheets are available<sup>31</sup>.

### 7.3 A symmetrical crack in a stiffened sheet

The Green's function used in the previous example can be used to examine the effect of detailed stiffener design<sup>32</sup>. The panel to be analysed is shown in Fig 17. This configuration represents a typical aircraft wing panel in which a crack is initiated at a rivet hole B and the tip A grows across the panel. The stiffeners of area  $A_s$  are attached to a sheet of thickness  $t$  at a spacing  $b$  with double rows of rivets, diameter  $d$ , having a pitch  $p$  perpendicular to the crack and a pitch  $h$  parallel to the crack; the modulus of elasticity of the sheet and the stiffener are identical. Typical values of  $p$ ,  $h$  and  $b$  together with relative area ratio  $A_s/(A_s + bt)$  are given on Fig 17. Since  $h$  is a significant fraction of the bay width  $b$ , it may be somewhat unrealistic to assume, in the analysis, that the stiffener can be concentrated along its centre line. This assumption will be compared with the more realistic one of concentrating half the total stiffener area along each rivet line. The computational problem is also made more complex because of the lack of symmetry; the crack is eccentrically placed and as only one tip moves the eccentricity changes. The stress intensity factors for crack tips A and B are shown in Fig 18 as a function of the crack length  $a$ . In the singly riveted model the stiffener area  $A_s$  is assumed concentrated along the stiffener centre line and in the doubly riveted model the area  $A_s$  is distributed equally along each rivet line. As can be seen the type of model assumed affects the stress intensity factor and hence the residual static strength<sup>33</sup>. The stress intensity factor is greater for the single row of rivets than for the double row for all values of  $a/(b - h/2)$  for tip B. For tip A the double row of rivets results in a smaller  $K_I$  than the single row for  $a/(b - h/2)$  between 1.03 and 1.33. The implications are that the residual strength and fatigue crack growth rate of the cracked panel will depend

strongly on the type of attachment, in this case single or double riveting. Therefore this must be taken into account in the analytic models used to solve these problems. It is interesting to note that for the doubly riveted stiffener model the critical crack tip alternates between tip A and tip B as the crack crosses the panel.

It is also possible to carry out simulated fatigue crack growth rate experiments using the computer. Both tips are allowed to move simultaneously; the increment of crack growth is determined from the fatigue crack growth law for the sheet material. Thus realistic comparisons of fatigue life can be made. Calculations with small crack increments can be time consuming; the Green's function technique makes it possible to use closed form expressions and thus solution times are shorter than for many numerical techniques.

## 8 CONCLUSIONS

The application of Green's function techniques in problems in fracture mechanics has been described. It has been shown to be a versatile technique for determining stress intensity factors in a wide variety of problems. Once the Green's function is known it is only necessary to determine the stress distribution along the crack site in the uncracked body. The stress analysis of uncracked bodies is, in general, simpler than the stress analysis of cracked bodies and many experimental and analytical techniques already exist. Some methods of obtaining new Green's functions from existing ones have been presented and further extensions indicated. Several commonly used approximate methods have been given a rational basis; they have been shown to depend on the existence of certain approximate Green's functions. Many important Green's functions have been collected and some of these have been used to solve practical problems in fracture mechanics. The range of problems included cracks at loaded holes, the load transfer in stiffeners due to attachment deflection, attachment failure and sheet yielding, and the effect of stiffener design on asymmetrically cracked panels. The Green's function technique is also applicable to problems in three-dimensions although applications are more limited at present because of the small number of Green's functions available.

## REFERENCES

- | <u>No.</u> | <u>Author</u>                                 | <u>Title, etc</u>   |
|------------|---|---|
| 1          | G.C. Sih (Ed)                                 | Methods of analysis and solutions of crack problems.<br><i>Mechanics of fracture</i> , Vol 1, Leyden, Noordhoff (1973)  |
| 2          | D.J. Cartwright<br>D.P. Rooke                 | Evaluation of stress intensity factors.<br>In <i>A general introduction to fracture mechanics</i> ,<br>pp 54-73, London, Mech. Engng. Publications (1978)   |
| 3          | D.P. Rooke<br>F.I. Baratta<br>D.J. Cartwright | Simple methods of determining stress intensity factors.<br>In <i>Practical applications of fracture mechanics</i> , edited<br>by H. Liebowitz, AGARDograph (to be published 1980)                           |
| 4          | G.E. Stedman                                  | Green's functions.<br><i>Contemp. Phys.</i> , 9, 49-69 (1968)   |
| 5          | P.C. Paris                                    | Stress analysis of cracks.<br>In <i>Fracture toughness and its applications</i> ,<br>STP 381, pp 30-83, ASTM (1965)   |
| 6          | H.F. Bueckner                                 | The propagation of cracks and the energy of elastic<br>deformation.<br><i>Trans ASME</i> , 80E, 1225-1230 (1958)  |
| 7          | H. Nisitani                                   | Solutions of notch problems by body force methods.<br>In <i>Stress analysis of notch problems, Mechanics of<br/>fracture</i> , Vol 5, edited by G.C. Sih, pp 1-68,<br>Alphen Aan Den Rijn, Noordhoff (1978) |
| 8          | F. Erdogan                                    | On the stress distribution in plates with collinear cuts<br>under arbitrary loads.<br><i>Proc. 4th US Nat. Congress of Applied Mechanics</i> ,<br>Vol 1, pp 547-553 (1962)                                  |
| 9          | R.J. Hartranft<br>G.C. Sih                    | Alternating methods applied to edge and surface crack<br>problems.<br>Chapter 4, pp 179-238 in Reference 1.   |
| 10         | D.P. Rooke<br>D.A. Jones                      | Stress intensity factors in fretting fatigue.<br><i>J. Strain Analysis</i> , 14, 1-6 (1979)   |
| 11         | H. Tada<br>P. Paris<br>G. Irwin               | <i>The stress analysis of cracks handbook</i> .<br>Hellertown, Pa., Del Research Corp. (1973)   |

REFERENCES (continued)

- | <u>No.</u> | <u>Author</u>                   | <u>Title, etc</u>   |
|------------|---------------------------------|---|
| 12         | D.P. Rooke<br>D.J. Cartwright   | <i>Compendium of stress intensity factors.</i><br>London, HMSO (1976)   |
| 13         | G.C. Sih                        | <i>Handbook of stress intensity factors.</i><br>Bethlehem, Pa., Lehigh University (1973)  |
| 14         | D.J. Cartwright                 | Stress intensity factors and residual static strength in certain structural elements.<br>PhD Thesis, Mech. Engng. Dept., University of Southampton (1971)                                     |
| 15         | J.G. Williams<br>D.P. Isherwood | Calculation of the strain energy release rates of cracked plates by an approximate method.<br><i>J. Strain Anal.</i> , <u>3</u> , 17-22 (1968)  |
| 16         | D.P. Rooke                      | Evaluation of asymptotic stress analysis for fracture mechanics applications.<br>RAE Technical Report 78074 (1978)  |
| 17         | R.C. Shah                       | Stress intensity factors for through and part-through cracks originating at fastener holes.<br>In <i>Mechanics of Crack Growth</i> , STP 590, pp 429-459, ASTM (1976)                         |
| 18         | R.C. Shah                       | On through cracks at interference fit fasteners.<br><i>J. Pressure Vessel Technology</i> , <u>99</u> , 75-82 (1977)   |
| 19         | T.M. Hsu<br>J.L. Rudd           | Green's function for thru-crack emanating from fastener holes.<br><i>Proc. 4th International Conf. on Fracture</i> , Vol 3, pp 139-148, Waterloo, Canada, University of Waterloo Press (1977) |
| 20         | R.S. Whitehead                  | BAe Warton (private communication)  |
| 21         | J. Tweed<br>D.P. Rooke          | The elastic problem for an infinite solid containing a circular hole with a pair of radial edge cracks of different lengths.<br><i>Int. J. Engng. Sci.</i> , <u>14</u> , 925-933 (1976)       |

REFERENCES (continued)

- | <u>No.</u> | <u>Author</u>                 | <u>Title, etc</u>  |
|------------|-------------------------------|--|
| 22         | E. Smith                      | Simple approximate methods for determining the stress intensification at the tip of a crack.<br><i>Int. J. Fracture</i> , <u>13</u> , 515-518 (1977)   |
| 23         | J. Tweed<br>D.P. Rooke        | The stress intensity factor for a crack at the edge of a loaded hole.<br><i>Int. J. Engng. Sci.</i> (to be published)  |
| 24         | J.M. Bloom<br>J.L. Sanders    | The effect of a riveted stringer on the stress in a cracked sheet.<br><i>J. Appl. Mech.</i> , <u>33</u> , 561-570 (1966)   |
| 25         | R. Greif<br>J.L. Sanders      | The effect of a stringer on the stress in a cracked sheet.<br><i>J. Appl. Mech.</i> , <u>32</u> , 59-66 (1965)   |
| 26         | C.C. Poe                      | Stress intensity factor for a cracked sheet with riveted and uniformly spaced stringers.<br>NASA TR R-358 (1971)   |
| 27         | T. Swift                      | The effects of fastener flexibility and stiffener geometry on the stress intensity in stiffened cracked sheets.<br><i>Proceedings of an International Conference on Prospects of Fracture Mechanics</i> , pp 419-436, Noordhoff (1974) |
| 28         | D.J. Cartwright<br>G. Dowrick | Effects of attachment deflection on fatigue crack growth rate of a crack in a stiffened sheet.<br><i>Fracture mechanics in engineering practice</i> , Ed. P. Stanley, pp 149-163, Applied Science (1977)                               |
| 29         | M.M. Ratwani                  | A parametric study of fatigue crack growth behaviour in adhesively bonded metallic structures.<br><i>Journal Engng. Materials Technology</i> , <u>100</u> , 46-51 (1978)   |
| 30         | K. Arin                       | A plate with a crack, stiffened by a partially debonded stringer.<br><i>Engng. fracture mechanics</i> , <u>6</u> , 133-140 (1974)  |
| 31         | D.J. Cartwright<br>T.P. Rich  | Plastic strip yielding for a crack in a stiffened sheet.<br><i>Proceedings of the International Conference on Numerical Methods in Fracture Mechanics</i> , Ed A.R. Luxmore and D.R.J. Owen, pp 550-568, Swansea University (1978)     |

REFERENCES (concluded)

<u>No.</u>	<u>Author</u>	<u>Title, etc</u>
32	K. Wang D.J. Cartwright	A crack near doubly riveted stiffeners. <i>Proceedings of the 4th International Conference on Fracture</i> , Vol 3, pp 647-656, Waterloo, Canada, University of Waterloo Press (1977)
33	W.G. Heath L.F. Nicholls W.T. Kirkby	Practical applications of fracture mechanics techniques to aircraft structural problems. In <i>Fracture mechanics design methodology</i> , AGARD conference proceedings No. 221 (1976)
34	M.K. Kassir G.C. Sih	Three dimensional crack problems. <i>Mechanics of fracture</i> , Vol 2, Leyden, Noordhoff (1975)

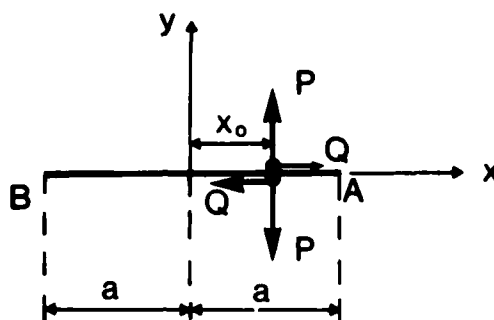


Fig 1 Crack loaded with point forces

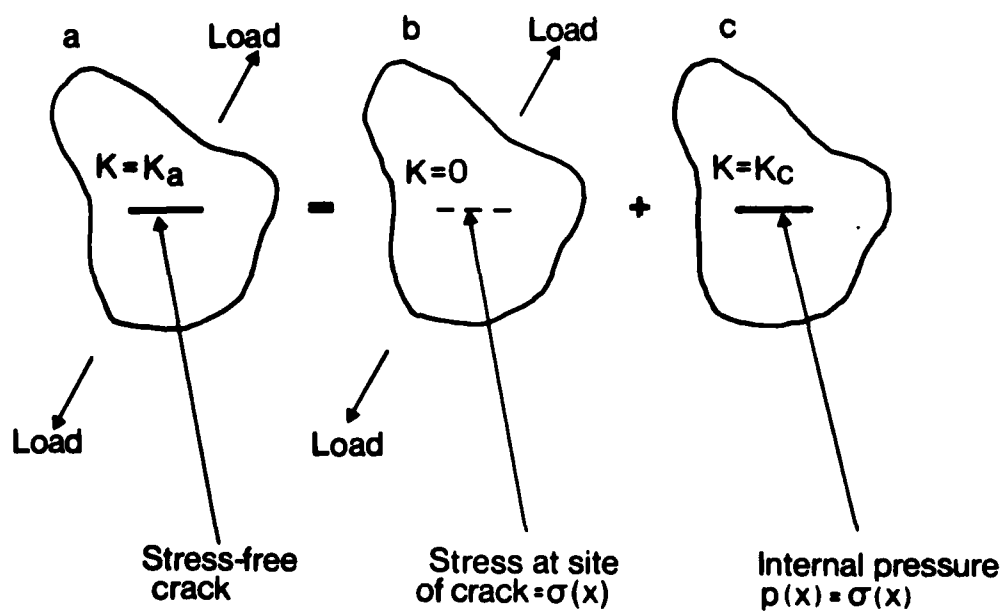


Fig 2 The equivalence of stress intensity factors for external boundary loads and internal pressures;  $K_a = K_c$

Fig 3

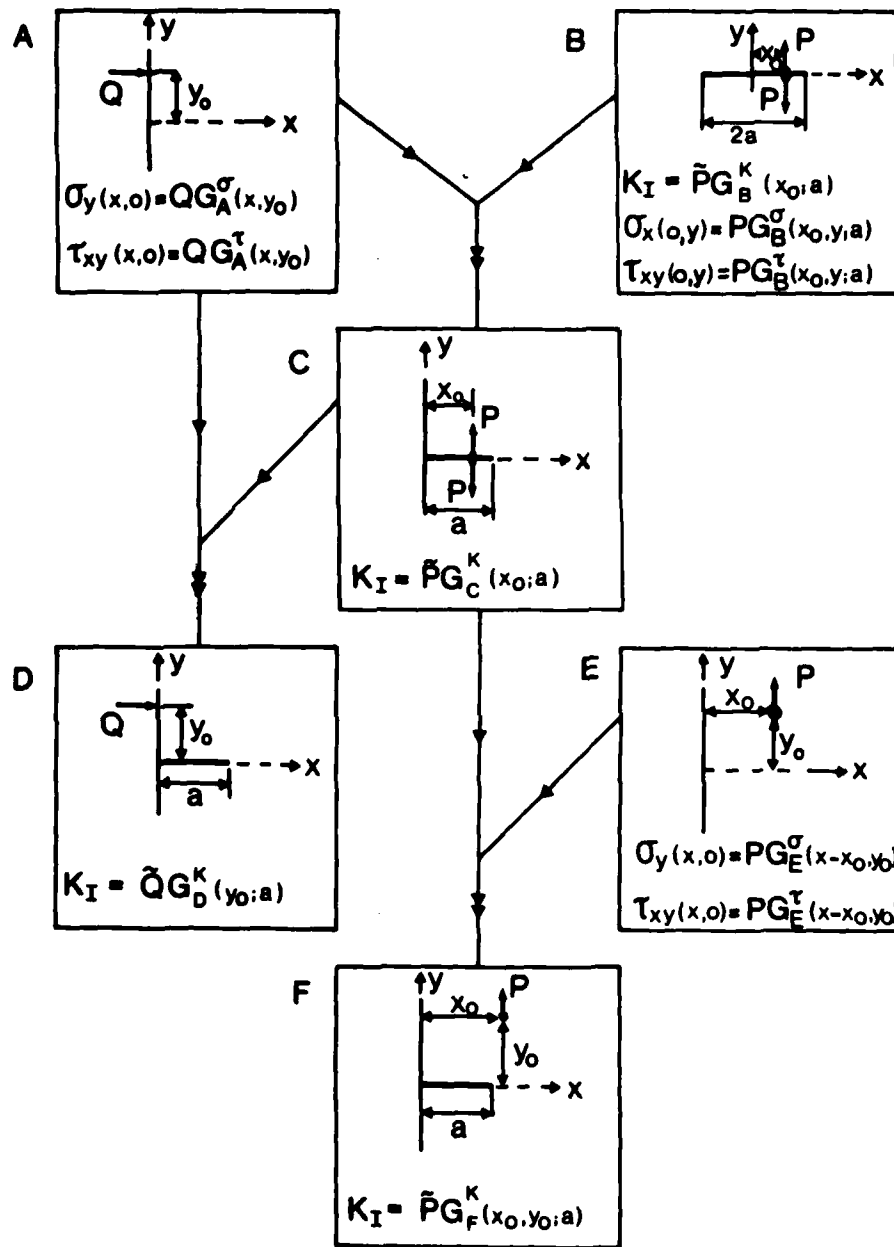


Fig 3 Systematic use of Green's functions  $\left[ \tilde{P} = P/(\sqrt{\pi a}), \tilde{Q} = Q/(\sqrt{\pi a}) \right]$

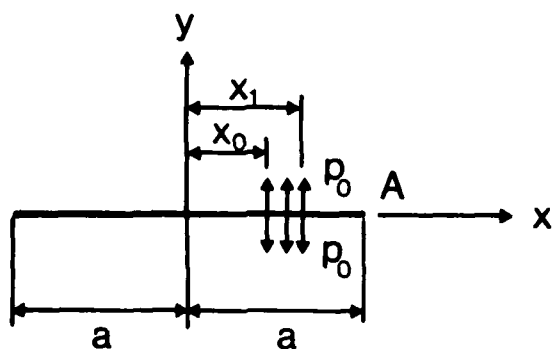


Fig 4a A step-pressure acting on the crack surface

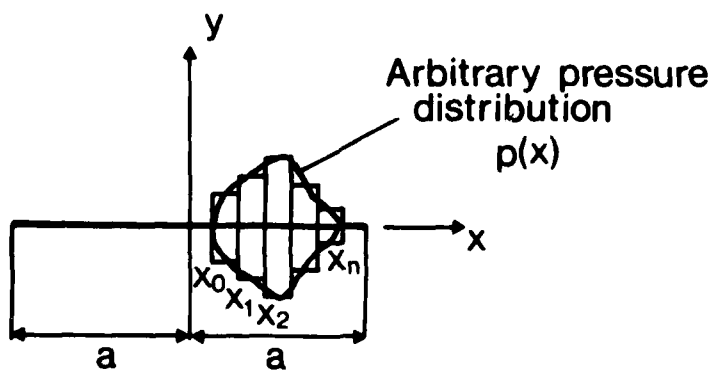
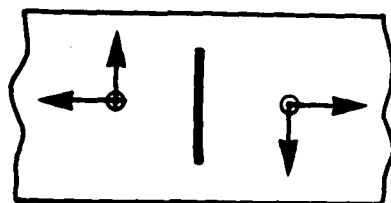
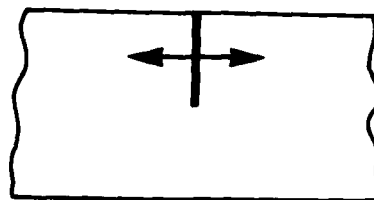


Fig 4b Step representation of a continuous pressure distribution

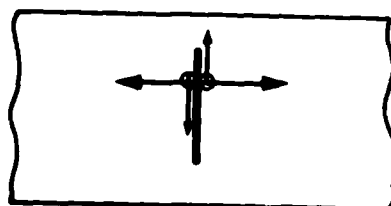
Fig 5a



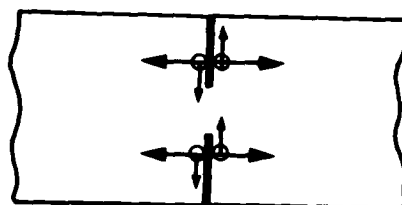
Central crack in strip  
[11]



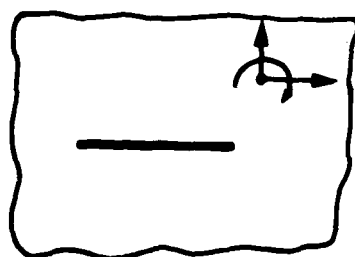
Edge crack in strip  
[11]



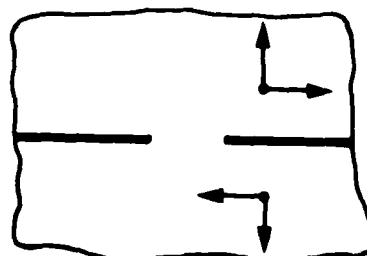
Central crack in strip  
[11]



Edge cracks in strip  
[11]



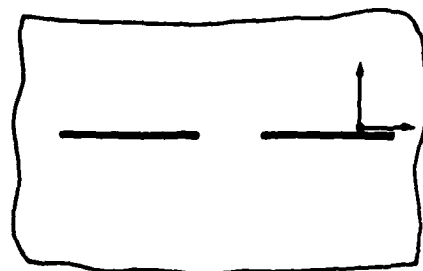
Crack in infinite sheet  
[11,12,13]



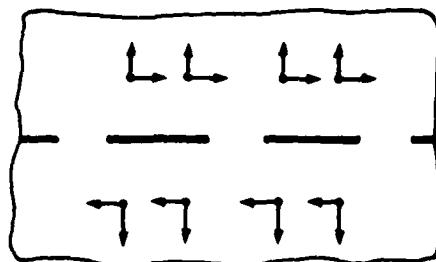
Two cracks in infinite  
sheet [11]

Fig 5a Configurations with known Green's functions

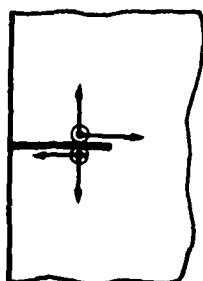
Fig 5b



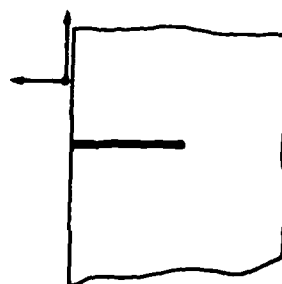
Two cracks in infinite sheet [11]



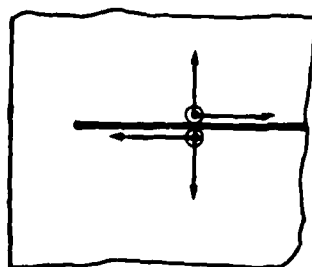
Array of cracks in infinite sheet [11]



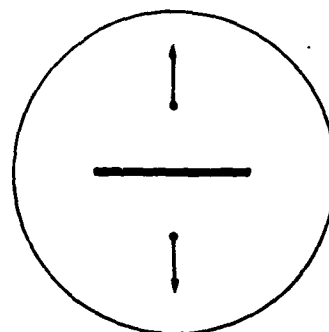
Edge crack in half-plane [11,13]



Edge crack in half-plane [10]



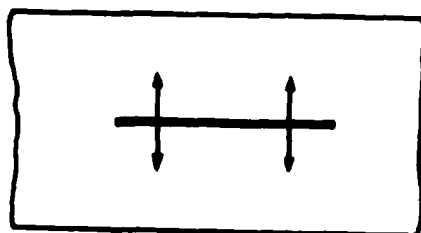
Crack near edge in half-plane [11]



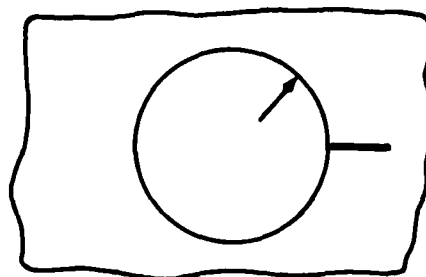
Crack in disc [11,12]

Fig 5b Configurations with known Green's functions

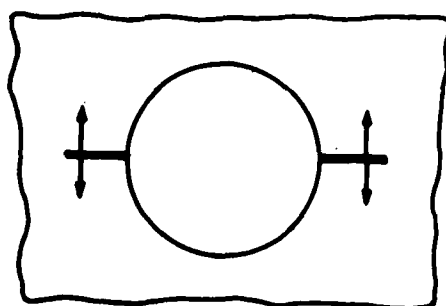
Fig 5c



Crack in strip [11]



Crack at hole [21]



Two cracks at hole [19]

Fig 5c Configurations with known Green's functions

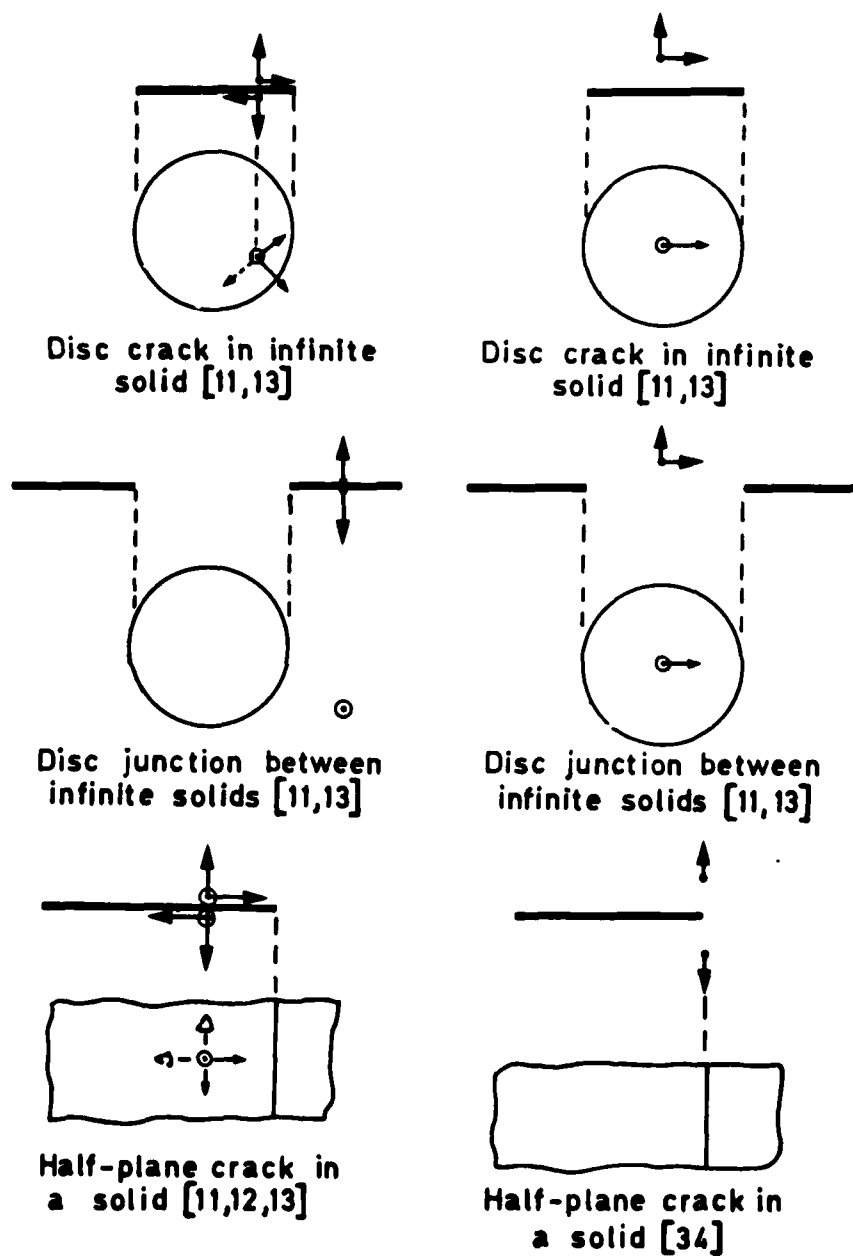


Fig 5d Configurations with known Green's functions

Fig 6

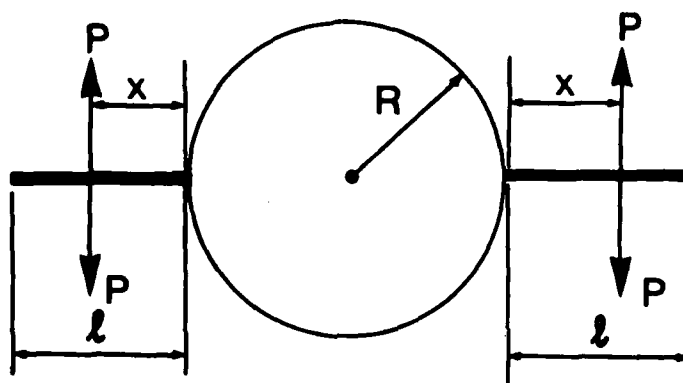


Fig 6 Diametrically opposed radial cracks subjected to symmetrical point forces

Fig 7

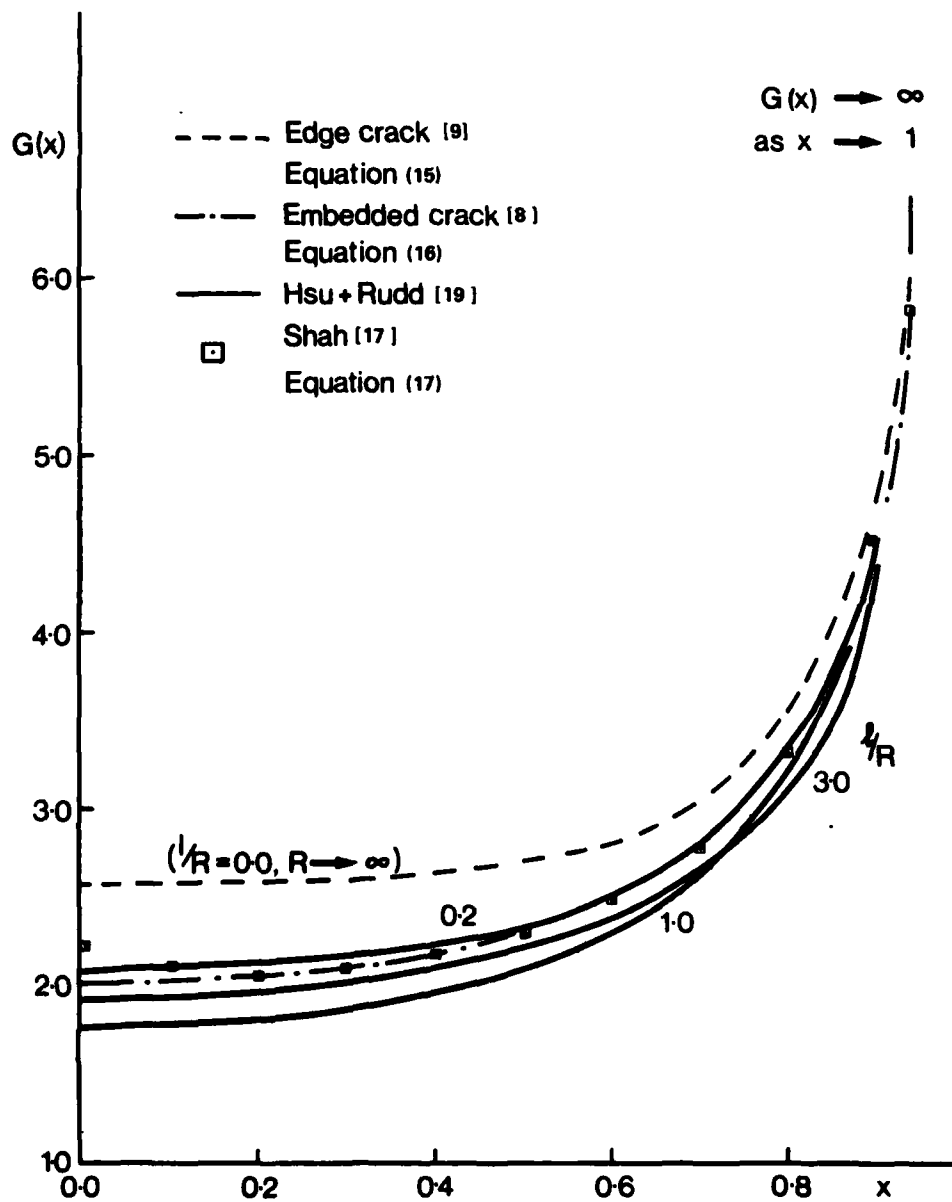


Fig 7 Comparison of Green's functions

Figs 8 & 9

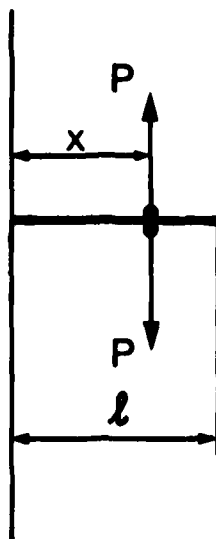


Fig 8 Point loaded crack emanating from a stress free edge

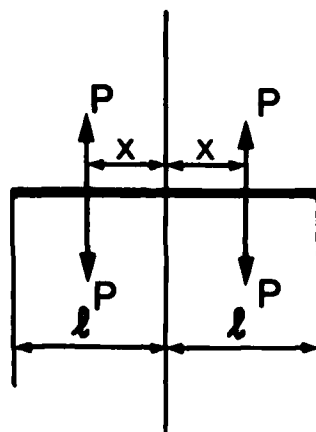


Fig 9 Point loaded crack embedded in an infinite sheet

Fig 10a&b

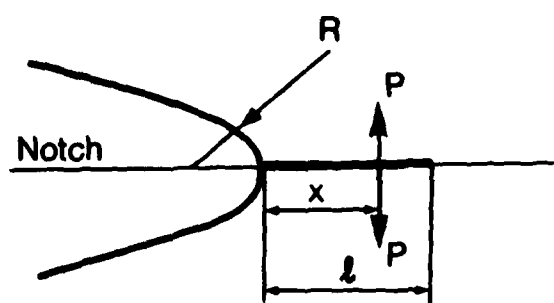


Fig 10a Point loaded crack at a notch root

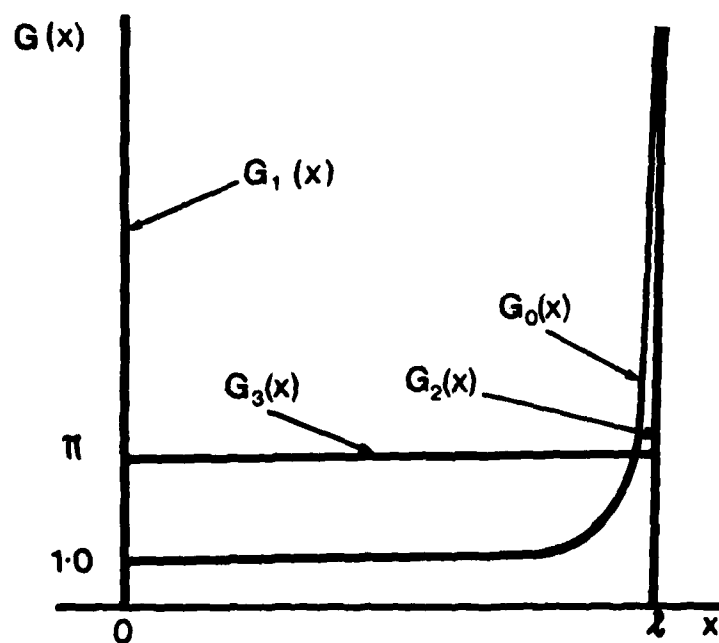


Fig 10b Schematic Green's functions for a crack at a notch root

Fig 11

$\frac{l}{R}$	Hsu and Rudd Reference 19	Tip stress Equation (24)	Maximum stress Equation (22)	Mean stress Equation (27)	Rooke and Tweed Reference 21
0.00	2.17 (-3.0)	2.24 (0)	2.24 (0)	2.24 (0)	2.24
0.10	1.99 (-0.5)	2.05 (+2.5)	2.24 (+12)	2.14 (+7)	2.00
0.15	1.90 (-0.5)	1.97 (+3)	2.24 (+17)	2.09 (+9)	1.91
0.20	1.83 (-0.5)	1.90 (+3)	2.24 (+22)	2.05 (+11)	1.84
0.30	1.70 (-1)	1.78 (+3.5)	2.24 (+30)	1.98 (+15)	1.72
0.50	1.54 (-1)	1.62 (+4)	2.24 (+44)	1.87 (+20)	1.56
1.00	1.34 (-2)	1.40 (+2)	2.24 (+64)	1.68 (+23)	1.37

Fig 11 Comparison of stress intensity factors  $K_I/(\sigma\sqrt{\pi l})$

Fig 12

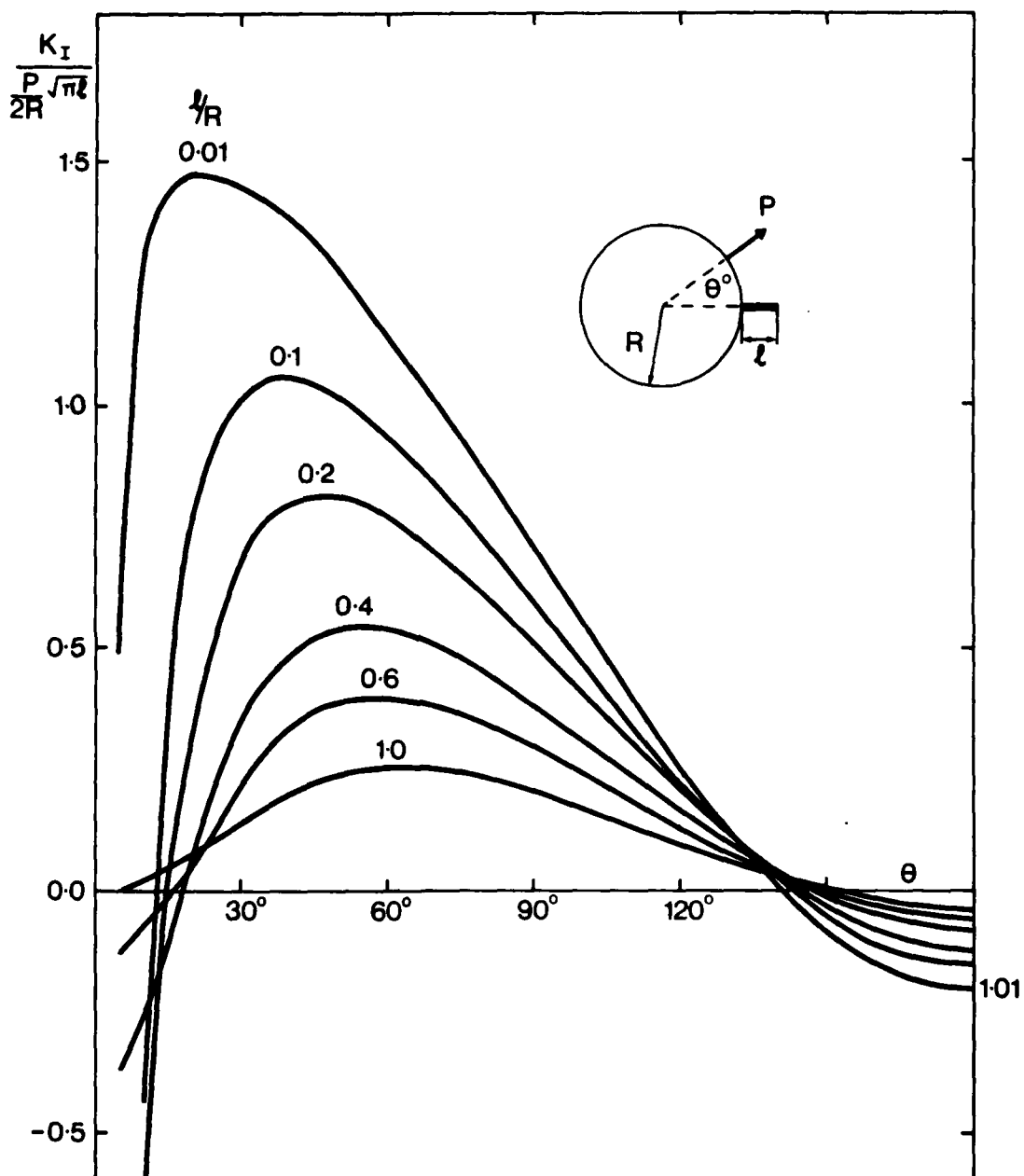


Fig 12 Green's function for a crack at the edge of a loaded circular hole

Fig 13

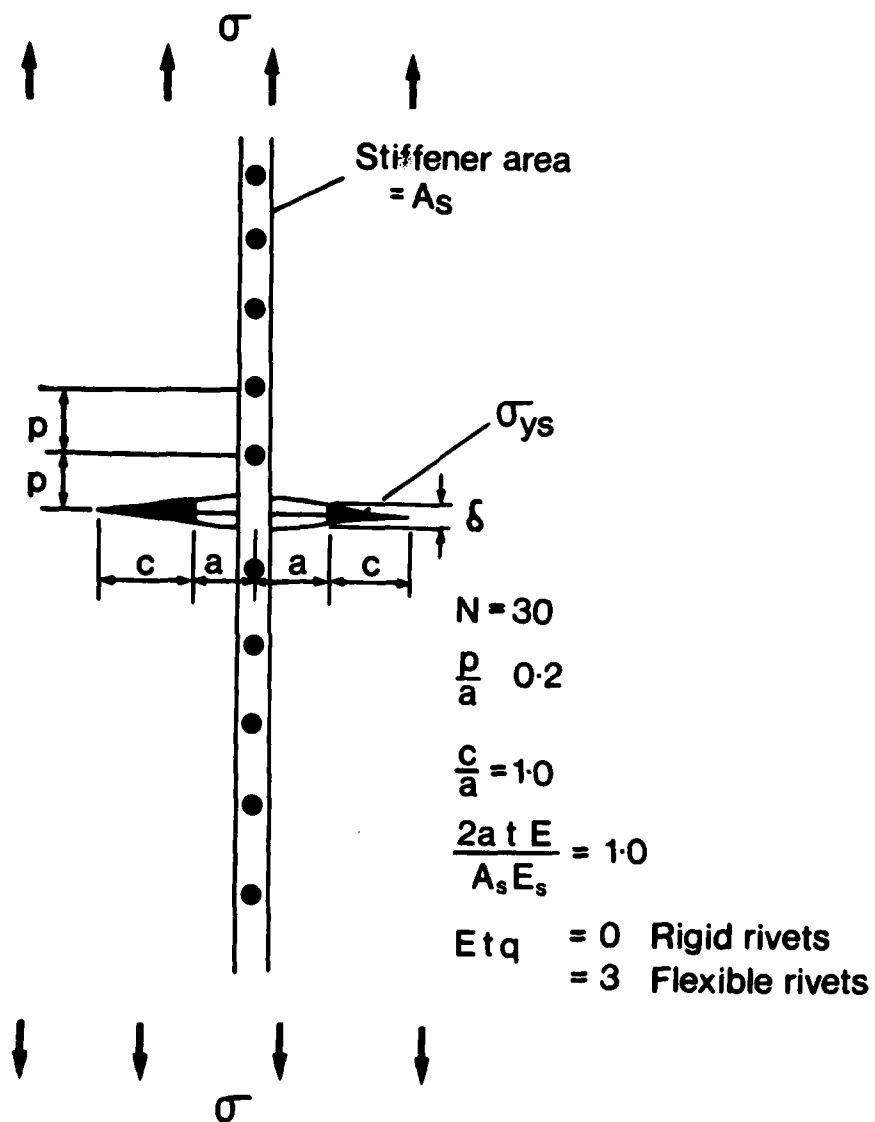


Fig 13 Strip yield crack at a riveted stiffener

Number of attachments failed	Strip-yield zone-ratio	Applied to yield stress ratio	COD ratio	Maximum stiffener stress ratio	Maximum rivet load ratio
$n$	$\frac{c}{c_0}$	$\frac{\sigma}{\sigma_s}$	$\frac{\delta}{\delta_0}$	$\frac{\sigma_m}{\sigma_s}$	$\frac{P_l}{\sigma_s A_s}$
0	0.367	0.827	0.356	1.596	0.269
2	0.451	0.799	0.438	1.499	0.287
4	0.547	0.770	0.545	1.400	0.252
6	0.638	0.745	0.651	1.317	0.208
8	0.716	0.726	0.738	1.252	0.169

Fig 14 Influence of attachment failure in a stiffened panel

$n$	$\frac{(\sigma_m)_{c=a}}{(\sigma_m)_{c=0}}$	$\frac{(P_l)_{c=a}}{(P_l)_{c=0}}$
0	1.06	1.09
1	1.06	1.11
2	1.07	1.14
3	1.07	1.18
4	1.07	1.22
5	1.07	1.26

Fig 15 Comparison of the maximum rivet load and the maximum stiffener stress for  $c = a$  and  $c = 0$

Fig 16

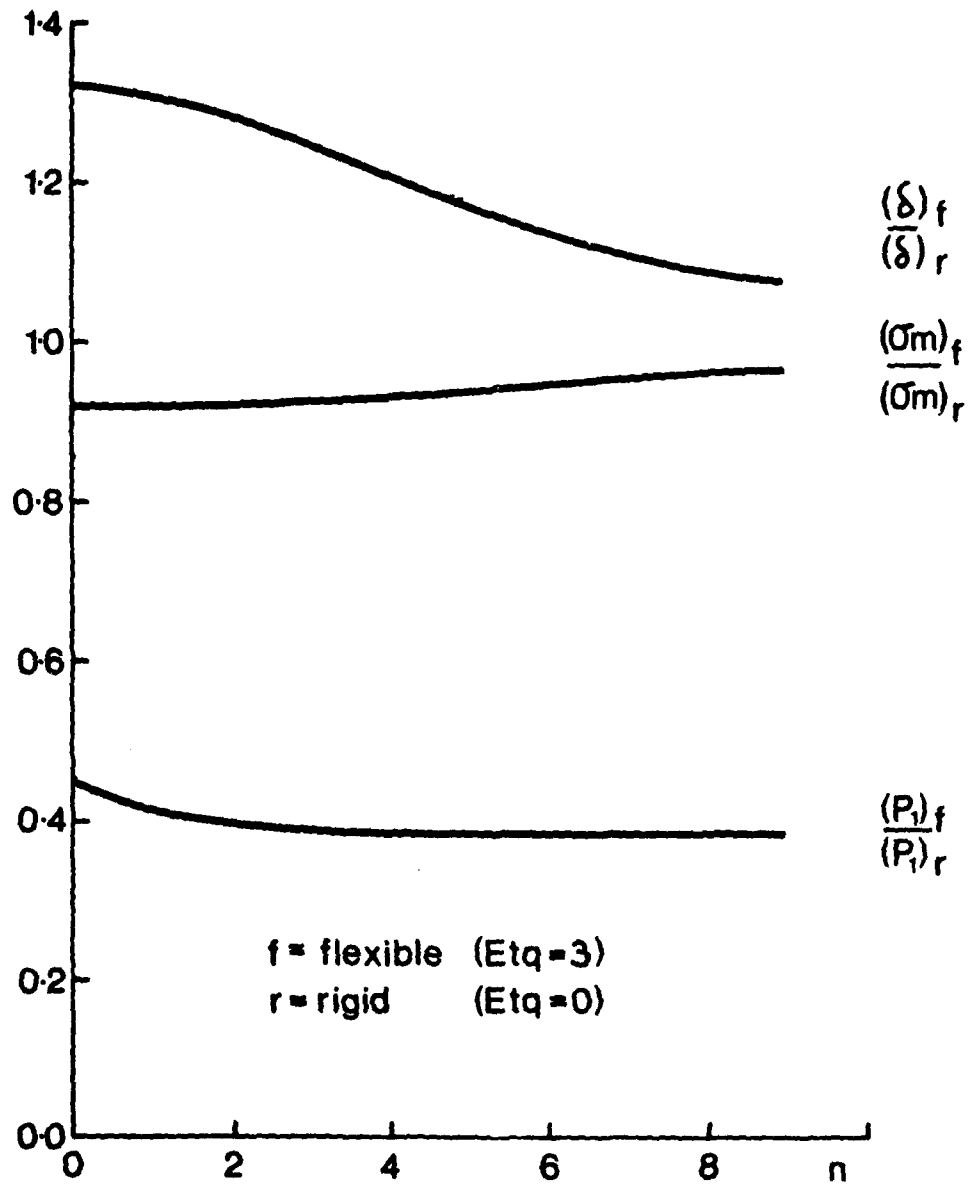


Fig 16 Effect of attachment shear deflection on maximum stiffener stress  $\sigma_m$ , maximum rivet load  $P_1$  and crack opening displacement  $\delta$

Fig 17

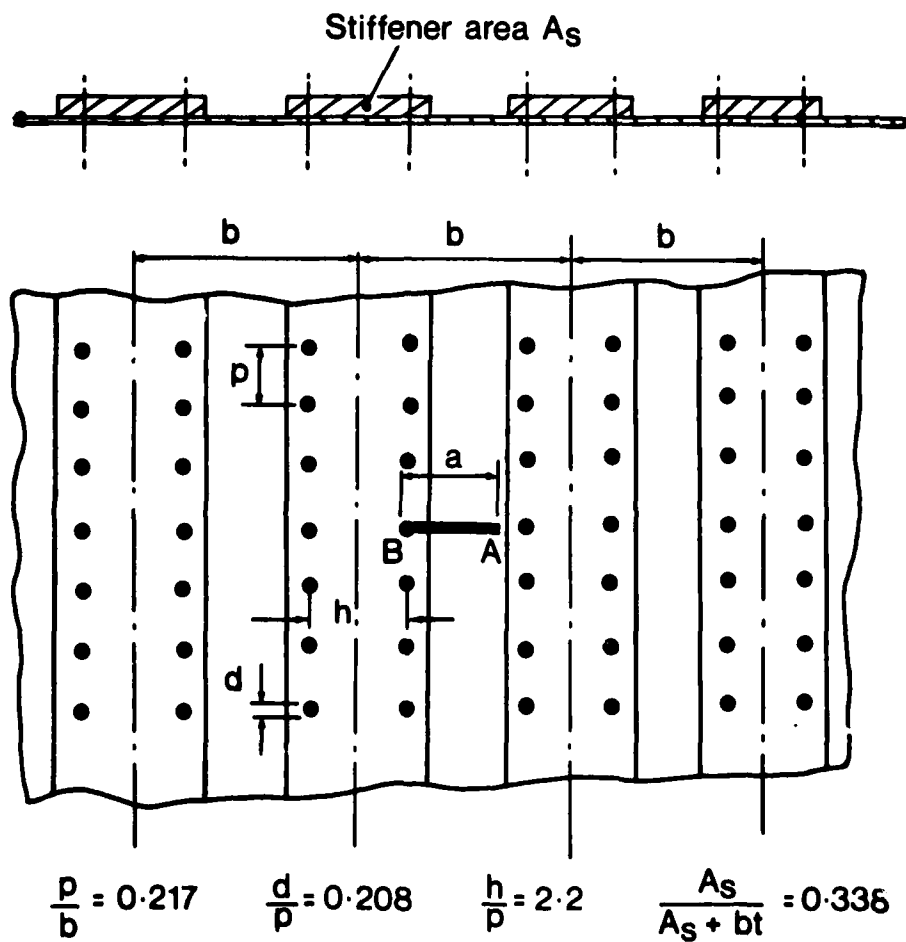


Fig 17 Cracked stiffened panel with tip B fixed at a rivet hole

Fig 18

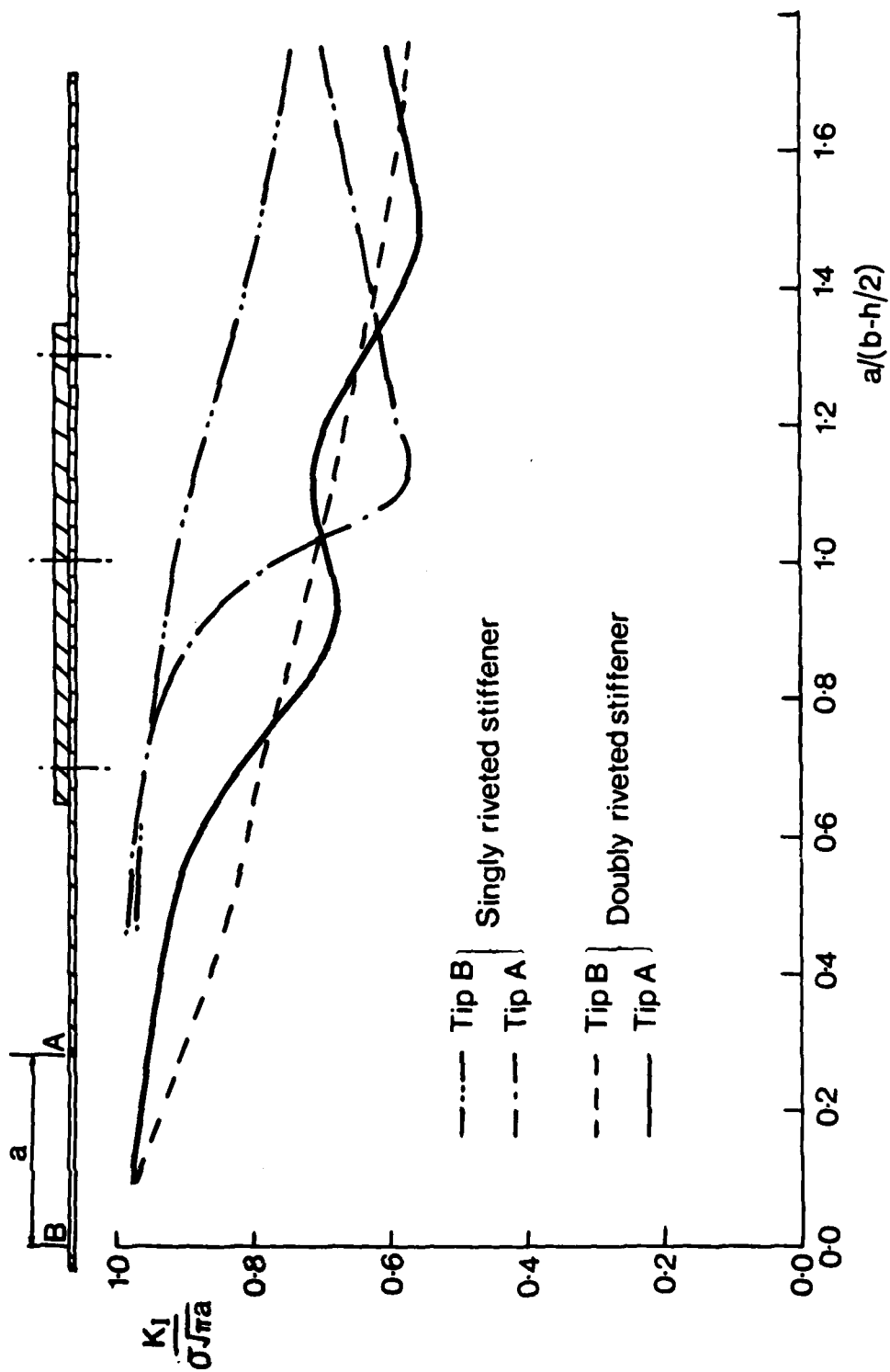


Fig 18 Comparison of stiffener rivet patterns on the stress intensity factor

# REPORT DOCUMENTATION PAGE

Overall security classification of this page

UNCLASSIFIED

As far as possible this page should contain only unclassified information. If it is necessary to enter classified information, the box above must be marked to indicate the classification, e.g. Restricted, Confidential or Secret.

1. DRIC Reference (to be added by DRIC)	2. Originator's Reference RAE TR 80035	3. Agency Reference N/A	4. Report Security Classification/Marking UNCLASSIFIED		
5. DRIC Code for Originator 7673000W		6. Originator (Corporate Author) Name and Location Royal Aircraft Establishment, Farnborough, Hants, UK			
5a. Sponsoring Agency's Code N/A		6a. Sponsoring Agency (Contract Authority) Name and Location N/A			
7. Title Green's functions in fracture mechanics					
7a. (For Translations) Title in Foreign Language					
7b. (For Conference Papers) Title, Place and Date of Conference Fracture Mechanics: Current Status, Future Prospects Conference at Cambridge, 16 March 1979					
8. Author 1. Surname, Initials Cartwright, D.J.	9a. Author 2 Rooke, D.P.	9b. Authors 3, 4 ....		10. Date March 1980	Pages 38
11. Contract Number N/A		12. Period N/A	13. Project	14. Other Reference Nos. Mat 394	
15. Distribution statement (a) Controlled by – ADXR (Mat) via DRIC (b) Special limitations (if any) –					
16. Descriptors (Keywords) (Descriptors marked * are selected from TEST) Fracture mechanics. Green's functions. Cracks*.					
17. Abstract → The use of Green's functions in the determination of stress intensity factors is described and applied to the solution of problems in fracture mechanics. Methods of obtaining further Green's functions from existing ones are presented. It is shown that several commonly used simple methods of determining stress intensity factors can be expressed in terms of approximate Green's functions. Many important Green's functions are presented and some of these are used to solve several problems of practical importance to the aerospace industry, eg cracks in stiffened sheets and cracks in pin-loaded lug-joints. ←					